A Robust and Sensitive Measurement for Sulcal Depth from Geometrical Approach

Hyuk Jin Yun, Kiho Im, Uicheul Yoon, Jin-Ju Yang, Jong-Min Lee

***Abstract*— Sulcal depth has been used for brain morphological analysis. Many previous approaches for measuring sulcal depth in cortical surfaces have been provided, but they have some limitations due to complex and convoluted sulcal geometry. We propose a novel algorithm for sulcal depth measurement, named adaptive distance transform (ADT). Reflecting sulcal geometry, ADT may be a sensitive method for brain atrophy and have robustness against sulcal variability. We demonstrate that ADT is sensitive approach by applying clinical data set. The group differences of mean sulcal depth between 25 patients with Alzheimer's disease (AD) and 25 normal controls using ADT and previous approaches (Euclidean and geodesic distance) are compared. The area under the receiver operating characteristic curve of three approaches is calculated for classifying performance of the algorithms. The area of receiver operating characteristic curve indicated that all three algorithms are sensitive measure to classifying subject into controls or AD. To compare robustness of algorithms, we designed simulation data set which is similar to sulcal shape. At the result, ADT has lower error than other algorithms estimated in simulation data. These results are discussed in terms of robust and sensitive measurement of ADT for sulcal depth.**

***Index Terms*— Sulcal Depth, Adaptive Distance Transform, Local coordinate, Simulation Data, Dijkstra's Algorithm**

I. Introduction

Several researchers in neuroimaging studies extract and analyze a various brain morphological features including curvature, fractal dimension, thickness, gyrification index, sulcal pit and sulcal depth based on the characteristics of brain which is a highly convoluted and folded structure [1-8]. Because the peculiarities of neurodegenerative diseases accompany changes of sulcal shape and cortical structure, these quantitative surface-based features have been largely used to study these diseases [1, 9, 10]. Among the various surface-based features, sulcal depth has been studied as an important index for cerebral health and widely used for brain morphological analysis [1, 8, 9, 11, 12]. We focused on sulcal depth because of two specific properties used in previous studies with brain morphology First, deep sulcal regions have robustness against inter-individual variability [13-15]. During development, the early major folds relate to genetic control and cytoarchitectonic areas, and they are quite consistent in the individuals [16, 17]. The brain morphological studies about development, asymmetry or brain size used sulcal depth as a consistent feature of cortical shape and deep sulcal region was thought to be a land mark [8, 11, 12, 18, 19]. Furthermore, because of robustness, deep sulcal landmarks such as sulcal- fundi, lines and pits were extracted by sulcal depth map [11, 14, 20, 21]. Second, sulcal depth has the sensitivity to cortical atrophy because it has been thought to be related with reduction of cortical thickness and gyral white matter volume [1]. So it has been used in several studies which analyzed the brain morphological changes caused by age-related trend, Williams syndrome, schizophrenia or Alzheimer's disease (AD) [1, 7, 10, 22]. These studies reported generally shallower patterns of sulcal depth related to cortical atrophy or disease progression.

Although different results are achieved through these different algorithms, sulcal depth is commonly defined as distance from the seed to cerebral sulci. All these previous algorithms for computing sulcal depth were mainly classified into two major approaches according to the definition of distance: Euclidean depth (EUD) and geodesic depth (GED).

Although both of EUD and GED have been used in neuroimaging studies as a sensitive or robust feature and showed clinically or methodologically significant results in brain morphology, they have some limitations on sulcal geometry. Disregarding degree of sulcal folding, the shortest path of EUD (Fig.1 (a)) could result in underestimated depth and erroneous deep sulcal region in case of convoluted shape of sulci. Degree of sulcal folding was fully reflected using GED (Fig.1 (b)), but there is other two limitations affected by position of seed points and detour characteristic. Gyral regions which are generally defined as seed point of GED have no automatical golden standard for extracting them. Therefore, the results of GED are variable depending on the position of the seed points. At the path around point D in fig.1 (b), another limitation, it had to make a detour along the surface instead of shorter path because of characteristic of GED, and this limitation can lead overestimated results and detect inaccurate deepest points. Point B, C and D in fig.1 describe the extreme cases of sulcus to explain the limitation of two major approaches; however, it is possible in practical brain structures.

Manuscript received June 27, 2012; revised August 10, 2012. This work was supported by the Korea Science and Engineering Foundation (KOSEF) NLRL program grant funded by the Korean Government (MEST) (2011-0028333) and Basic Science Research Program through the National Research Foundation of Korea (NRF) funded by the Ministry of Education, Science and Technology(MEST)(2011-0014862).

Hyuk Jin Yun is with the Department of Biomedical Engineering, Hanyang University, Seoul, South Korea (e-mail: yunhj@bme.hanyang.ac.kr).

Kiho Im was with Department of Biomedical Engineering, Hanyang University, Seoul, South Korea. He is now with the Division of Newborn Medicine, Children's Hospital Boston, Harvard Medical School, Boston, MA, 02115, USA, Center for Fetal Neonatal Neuroimaging and the Developmental Science, Children's Hospital Boston, Harvard Medical School, Boston, MA, USA (e-mail: kiho.sky@gmail.com).

Uicheul Yoon was with Department of Biomedical Engineering, Hanyang University, Seoul, South Korea. He is now with the Department of Biomedical Engineering, College of Health and Medical Science, Catholic University, Daegu, South Korea (e-mail: yoonuc@gmail.com).

Jin-ju Yang is with the Department of Biomedical Engineering, Hanyang University, Seoul, South Korea (e-mail: jinju@bme.hanyang.ac.kr).

Jong-Min Lee (corresponding author to provide phone: +82-2-2220-0697; fax: +82-2-2296-5943; e-mail: ljm@hanyang.ac.kr) is with the Department of Biomedical Engineering, Hanyang University, Seoul, South Korea.

ISBN: 978-988-19252-4-4
ISSN: 2078-0958 (Print); ISSN: 2078-0966 (Online)

As we mentioned above, these two algorithms can drive under/overestimation of sulcal depth in some cases. Changes of cortical structure including sulcus undergo various influences like genetic factors, neurodegenerative diseases or aging, so it is important that the algorithm for sulcal depth should be more sensitive of morphological change and robust for sulcal variability. In this paper, we suggested a novel algorithm, named adaptive distance transform (ADT), a sensitive and robust algorithm for computing sulcal depth. It is described in fig.1 (c), defined as the shortest path from outer convex hull to vertices in cortical surface following the sulcal geometry. We describe ADT using Dijkstra's algorithm that is a graph searching algorithm that find shortest path from source. The strong point of ADT is reflection of geometrical properties form highly convoluted and folded structure of sulci. This may be beneficial in studies of brain morphology. We compared the sulcal depth computed using ADT with EUD and GED in terms of the robustness and sensitivity.

II. MATERIALS AND METHODS

A. Participants

Fifty right-handed subjects (aged 65-96 yr) were selected from the Open Access Series of Imaging Studies (OASIS) database (http://www.oasis-brains.org). OASIS cross-sectional data set has a collection of 416 subjects aged 18 to 96 including individuals with demented older adults. For this study, we selected data from all 28 AD patients whose clinical dementia rating (CDR) of 1 and three of them failed in image processing were excluded. The 25 subjects with CDR of 0 are randomly selected. Finally, there are 25 subjects who have been diagnosed with AD and 25 non-demented. A summary of subject demographics is shown in table 1.

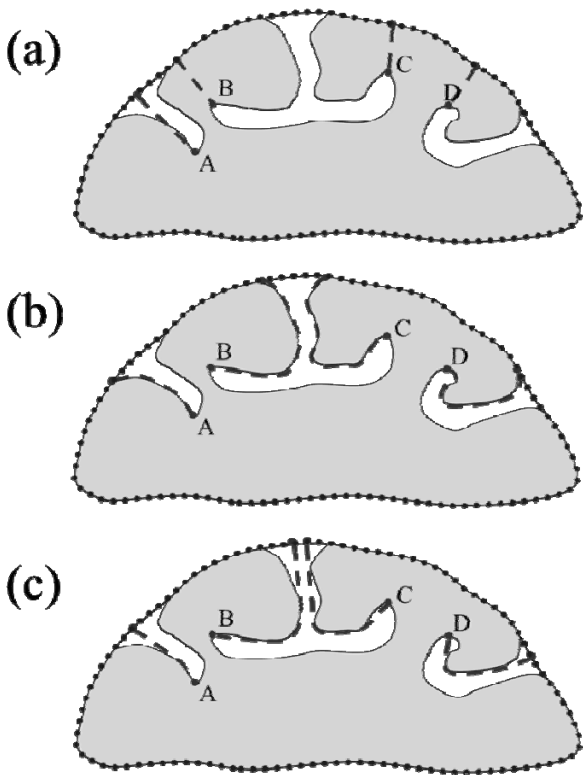

Fig. 1. An illustration of algorithms for computing sulcal depth : (a) EUD, (b) GED, (c) ADT. The dash lines illustrate distance paths of each approach and the dotted lines denote convex hull i.e. seed of depth.

Table 1
Demographic characteristics of subjects

	NC (n=25)	mild AD (n=25)
Age	74.88 (86-66)	77.76 (96-65)
Gender	8 males, 17 females	8 males, 17 females
CDR	0	1
MMSE score	28.56 (25-30)	21.52 (15-29)
Years of education	2.84 (1-5)	2.6 (1-5)

B. Image Processing

T1-weighted images were processed using CIVET pipeline with registration to ICBM-152 template using a linear transformation and correction for intensity nonuniformity in the magnetic field [24, 25]. The corrected and registered volumes were classified into white matter, gray matter, cerebrospinal fluid and background using an advanced neural net classifier [26]. The surfaces of the inner and outer cortex were automatically extracted using the Constrained Laplacian-Based Automated Segmentation with Proximities (CLASP) algorithm [27]. The reconstructed hemispheric cortical surfaces consisted with 40,962 vertices each forming high-resolution meshes.

.

C. Local coordinate

The implementation of ADT on cortical surfaces needs convex hull and local coordinate. Local coordinate refers to Cartesian coordinate between convex hull and cortical surface model[20]. We constructed convex hull on volume images that has been used by several previous studies [1, 12]. We made masked volume image isolating the voxels in the surface. The masked image was binarized and performed 3-d morphological closing operation with 10mm spherical kernel which could fill up the sulci [1, 12]. The Laplacian of Gaussian mask was used to construct a convex hull from closed image. On volume images, local coordinate which is the restricted regions between convex hull and cortical surface model were represented in voxel dimension. We used the closed volume image and cortical surface to construct local coordinate. Similar to the masked image, the voxels inside the surface were eliminated from closed image. The remained voxels become the local coordinate, which has 1mm isotropic level according to our data set. We divided local coordinate to 0.5 mm level for improving accuracy of ADT.

D. Adaptive distance transform

The basic idea of ADT is applying Dijkstra's algorithm to local coordinate. It computes the minimal cost of reaching any node on a network that solves the single-source shortest path problem for a graph with nonnegative edge path costs, producing a shortest path. For a rectangular network, the minimal total cost U_{ij} of reaching at the node x_{ij} can be written in terms of the minimal total cost of reaching at its neighbors [28]:

ISBN: 978-988-19252-4-4
ISSN: 2078-0958 (Print); ISSN: 2078-0966 (Online)

$$U_{ij} = \min\left(U_{i-1,j}, U_{i+1,j}, U_{i,j-1}, U_{i,j+1}\right) + C_{ij} \dots\dots\dots\dots [1]$$

To find the minimal total cost, it separates nodes into three classes: 'Far' (no information about U), 'Accepted' (U has been computed), and 'Considered' (neighborhood of 'Accepted'). The algorithm changes 'Considered' x_{ij} into 'Accepted' set and its 'Far' neighbors into the 'Considered' set. All nodes on network were changed to 'Accepted' set according to Eq. [1].

Our approach is different from that of classic Djikstra's algorithm which has prior information of edge and cost. Because the points of local coordinate do not have any information of 'Considered' nodes and cost around 'Accepted' nodes, we searched temporary 'Considered' nodes and calculated temporary cost around 'Accepted' nodes. Each node located inside the 26-neighborhood of an 'Accepted' node is classed as 'Considered' node and the EUD distance between the 'Accepted' node and each 'Considered' nodes becomes a cost. In case of ADT, the modified Eq. [1] is

$$U_{ijk} = \min\left(U_{ijk_n} + C_{ijk_n}\right) \dots\dots\dots\dots [2]$$

The U_{ijk_n} denotes the minimal total cost of n th neighborhood of x_{ijk} from convex hull (starting nodes) and C_{ijk_n} means the cost between U_{ijk_n} and U_{ijk}. Detailed procedures of ADT algorithm are explained as follows:

(1) Set the U of local coordinate to infinity and convex hull ('Accepted') to 0.
(2) Find an 'Accepted' node x_{ijk}.
(3) Search the temporary 'Considered' nodes around (2) and calculate C_{ijk_n}.
(4) Apply Eq. [2] to the node (2).
(5) Repeat (2) through (4) all points in local coordinate until all U do not change any more.

E. Computing EUD and GED

To compare with the other depth algorithms, we compute EUD and GED in our data set. We implemented these two algorithms for sulcal depth calculated on all the vertices in cortical surface as previous studies [12, 29].

F. Simulation data

The locations of deepest points of sulci could be defined by sulcal depth map, but they have spatial variability according to measuring algorithms. In case of complicated sulcus, some algorithms could detect mistaken location because of their limitations. For that reason, we made simulation data set which is similar to real sulcal shape to analyze the robustness, and whose location of deepest point is easily defined. We assumed for simulated data set that there are three components - sulcal width(w), folding degree(θ) and length(l) of medial line of sulcus, contribute to define sulcal morphology, then we designed 56 simulation data changing these components.

The simulation data set was constructed first in volume image, then anatomic segmentation using proximities algorithm minimizing objective functions [30] was performed to extract to surface models of simulation data set consisting of 20,480 discrete triangular elements (10,242 vertices). Finally, we defined the deepest point(d) as an end point of medial line and measure depth on simulation data set.

G. Data analysis

The receiver operating characteristic (ROC) curve for normal control and AD groups was performed as a measure of performance of classifying subject into controls or AD.

Since the algorithms have different paths and indicate dissimilar location of deep sulcal regions in even same subject depended by their properties, we compared the robustness using simulation data set. For evaluating the robustness of each algorithm, we estimated the errors between depth of deepest point(d) and deepest depth measured by each algorithm in simulation data set. The errors on simulation data were categorized and averaged by components.

III. Results

We compared sensitivity to cortical atrophy of ADT and other algorithm using clinical data set. ROC curve for all three algorithms are shown in fig. 2. The AUC values were as follows: ADT 0.8176, EUD 0.8344 and GED 0.7024.

The performance errors for 56 simulated sulci and a range of the each component are plotted in Fig. 3. Within all of the range of the components shown, the ADT algorithm exhibited lower error rates than EUD and GED. In general, the error consistently rose in all three algorithms as the values of components were increased. However, for ADT the error rate was increased slightly while EUD and GED produced dramatically higher error rate.

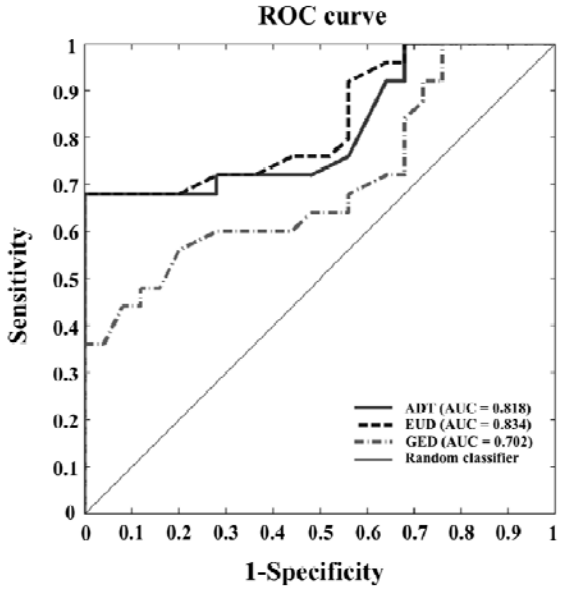

Fig. 2. ROC curves which are plots of sensitivity and specificity of algorithms for distinguish normal controls from patients with mild AD. AUCs are added in the figure.

IV. Discussion

We suggested a novel sulcal depth measuring algorithm named ADT to overcome the limitations of the EUD and GED, which were defined as the shortest path from cortical surface to outer convex hull following the sulcal geometry. The basic theory of ADT algorithm is applying Dijkstra's

ISBN: 978-988-19252-4-4
ISSN: 2078-0958 (Print); ISSN: 2078-0966 (Online)

algorithm to local coordinate and the path of depth is different from previous approach (Fig .1).

In the previous studies, deep sulcal region has been used to sulcal landmark because of their robustness against sulcal geometry[8, 11, 12, 18, 19]. The robustness could be compared the location of the deepest points in sulci, but there was no absolute standard of them. Therefore, simulation data set was designed to analyze the robustness. The averaged error of ADT was lower and more consistent than other algorithms. Especially the ADT algorithm had a low effect and constant error rate on component 'degree' while EUD and GED produce extremely large errors. The component 'degree' was assumed how complicated and convoluted sulcus had. In other words, it could be interpreted that ADT is independent to sulcal complexity and had superior robustness than other algorithms. It can be explained by its property reflecting sulcal geometry. The robustness of sulcal depth against sulcal variability could influence to extract deep sulcal landmarks like sulcal pits, fundi and lines in highly convoluted and folded structure of sulci. Ultimately in case of robustness, we suggest ADT as a powerful method in brain morphological study.

Brain atrophy changes that occur on the pial surface could decrease the sulcal depth. Many previous studies which investigated age- or disease- related changes in sulcal depth as a sensitive feature of brain atrophy using EUD and GED algorithms have been reported significant difference between the control group and the AD patient group [1, 4, 22]. In terms of distinction controls from AD patients, the AUC analysis suggested that ADT and EUD algorithms were "good" tests but GED was a "fair" test. Our results explained that the ADT algorithm could be a sensitive measure computing sulcal depth. There are two reasons why

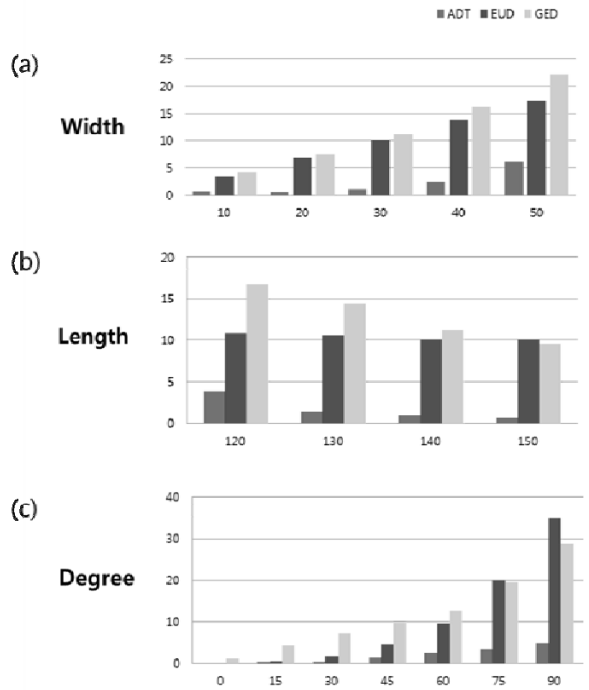

Fig. 3. Average normalized difference of each algorithm in simulation data set. Normalized difference measured by following difference rate equation : abs((largest value - depth of d)/(depth of d))×100.

sensitivity of sulcal depth was little affected by algorithm. First in pial surfaces, sulcus is very narrow structure and most of sulci have simple shape. Because of this, the path of depth little difference to represent their sensitive property. Furthermore, the mean sulcal depth can distort the effect of different path. Gyral regions and sulcal wall included within calculation of mean sulcal depth in this study thought to be nonsensical regions. Some previous studies with sulcal depth [1, 8]defined sulcal regions from sulcal depth map due to eliminating effects of nonsensical region. However, in this study, it is hard to define sulcal regions from previous studies. The sensitivity of sulcal depth may be needed for more exact analysis method between groups in future work.

Finally, the results of this study say that ADT is more robust algorithm than previous algorithms and have enough sensitivity for cortical atrophy and diagnosis of AD. It is our hope that ADT algorithm will use morphometric and clinical analysis to provide better results.

REFERENCES

[1] K. Im, J. M. Lee, S. W. Seo, S. Hyung Kim, S. I. Kim, and D. L. Na, "Sulcal morphology changes and their relationship with cortical thickness and gyral white matter volume in mild cognitive impairment and Alzheimer's disease," *Neuroimage,* vol. 43, pp. 103-13, Oct 15 2008.

[2] K. Im, J. M. Lee, J. Lee, Y. W. Shin, I. Y. Kim, J. S. Kwon, and S. I. Kim, "Gender difference analysis of cortical thickness in healthy young adults with surface-based methods," *Neuroimage,* vol. 31, pp. 31-8, May 15 2006.

[3] J. P. Lerch and A. C. Evans, "Cortical thickness analysis examined through power analysis and a population simulation," *Neuroimage,* vol. 24, pp. 163-73, Jan 1 2005.

[4] V. A. Magnotta, N. C. Andreasen, S. K. Schultz, G. Harris, T. Cizadlo, D. Heckel, P. Nopoulos, and M. Flaum, "Quantitative in vivo measurement of gyrification in the human brain: changes associated with aging," *Cereb Cortex,* vol. 9, pp. 151-60, Mar 1999.

[5] T. White, N. C. Andreasen, P. Nopoulos, and V. Magnotta, "Gyrification abnormalities in childhood- and adolescent-onset schizophrenia," *Biol Psychiatry,* vol. 54, pp. 418-26, Aug 15 2003.

[6] R. D. King, B. Brown, M. Hwang, T. Jeon, and A. T. George, "Fractal dimension analysis of the cortical ribbon in mild Alzheimer's disease," *Neuroimage,* vol. 53, pp. 471-9, Nov 1 2010.

[7] J. S. Kippenhan, R. K. Olsen, C. B. Mervis, C. A. Morris, P. Kohn, A. Meyer-Lindenberg, and K. F. Berman, "Genetic contributions to human gyrification: sulcal morphometry in Williams syndrome," *J Neurosci,* vol. 25, pp. 7840-6, Aug 24 2005.

[8] D. C. Van Essen, "A Population-Average, Landmark- and Surface-based (PALS) atlas of human cerebral cortex," *Neuroimage,* vol. 28, pp. 635-62, Nov 15 2005.

[9] B. I. Turetsky, P. Crutchley, J. Walker, R. E. Gur, and P. J. Moberg, "Depth of the olfactory sulcus: a marker of early embryonic disruption in schizophrenia?," *Schizophr Res,* vol. 115, pp. 8-11, Nov 2009.

[10] D. C. Van Essen, D. Dierker, A. Z. Snyder, M. E. Raichle, A. L. Reiss, and J. Korenberg, "Symmetry of cortical folding abnormalities in Williams syndrome revealed by surface-based analyses," *J Neurosci,* vol. 26, pp. 5470-83, May 17 2006.

[11] K. Im, H. J. Jo, J. F. Mangin, A. C. Evans, S. I. Kim, and J. M. Lee, "Spatial distribution of deep sulcal landmarks and hemispherical asymmetry on the cortical surface," *Cereb Cortex,* vol. 20, pp. 602-11, Mar 2010.

[12] K. Im, J. M. Lee, O. Lyttelton, S. H. Kim, A. C. Evans, and S. I. Kim, "Brain size and cortical structure in the adult human brain," *Cereb Cortex,* vol. 18, pp. 2181-91, Sep 2008.

[13] G. Lohmann, D. Y. von Cramon, and H. Steinmetz, "Sulcal variability of twins," *Cereb Cortex,* vol. 9, pp. 754-63, Oct-Nov 1999.

[14] G. Lohmann, D. Y. von Cramon, and A. C. Colchester, "Deep sulcal landmarks provide an organizing framework for human cortical folding," *Cereb Cortex,* vol. 18, pp. 1415-20, Jun 2008.

ISBN: 978-988-19252-4-4
ISSN: 2078-0958 (Print); ISSN: 2078-0966 (Online)

[15] G. Le Goualher, E. Procyk, D. L. Collins, R. Venugopal, C. Barillot, and A. C. Evans, "Automated extraction and variability analysis of sulcal neuroanatomy," *IEEE Trans Med Imaging,* vol. 18, pp. 206-17, Mar 1999.
[16] P. Rakic, "Specification of cerebral cortical areas," *Science,* vol. 241, pp. 170-6, Jul 8 1988.
[17] I. H. Smart and G. M. McSherry, "Gyrus formation in the cerebral cortex of the ferret. II. Description of the internal histological changes," *J Anat,* vol. 147, pp. 27-43, Aug 1986.
[18] A. Fornito, S. J. Wood, S. Whittle, J. Fuller, C. Adamson, M. M. Saling, D. Velakoulis, C. Pantelis, and M. Yucel, "Variability of the paracingulate sulcus and morphometry of the medial frontal cortex: associations with cortical thickness, surface area, volume, and sulcal depth," *Hum Brain Mapp,* vol. 29, pp. 222-36, Feb 2008.
[19] M. D. Cykowski, O. Coulon, P. V. Kochunov, K. Amunts, J. L. Lancaster, A. R. Laird, D. C. Glahn, and P. T. Fox, "The central sulcus: an observer-independent characterization of sulcal landmarks and depth asymmetry," *Cereb Cortex,* vol. 18, pp. 1999-2009, Sep 2008.
[20] C. Y. Kao, M. Hofer, G. Sapiro, J. Stem, K. Rehm, and D. A. Rottenberg, "A geometric method for automatic extraction of sulcal fundi," *IEEE Trans Med Imaging,* vol. 26, pp. 530-40, Apr 2007.
[21] J. K. Seong, K. Im, S. W. Yoo, S. W. Seo, D. L. Na, and J. M. Lee, "Automatic extraction of sulcal lines on cortical surfaces based on anisotropic geodesic distance," *Neuroimage,* vol. 49, pp. 293-302, Jan 1 2010.
[22] P. Kochunov, J. F. Mangin, T. Coyle, J. Lancaster, P. Thompson, D. Riviere, Y. Cointepas, J. Regis, A. Schlosser, D. R. Royall, K. Zilles, J. Mazziotta, A. Toga, and P. T. Fox, "Age-related morphology trends of cortical sulci," *Hum Brain Mapp,* vol. 26, pp. 210-20, Nov 2005.
[23] K. Im, J. M. Lee, U. Yoon, Y. W. Shin, S. B. Hong, I. Y. Kim, J. S. Kwon, and S. I. Kim, "Fractal dimension in human cortical surface: multiple regression analysis with cortical thickness, sulcal depth, and folding area," *Hum Brain Mapp,* vol. 27, pp. 994-1003, Dec 2006.
[24] D. L. Collins, P. Neelin, T. M. Peters, and A. C. Evans, "Automatic 3D intersubject registration of MR volumetric data in standardized Talairach space," *J Comput Assist Tomogr,* vol. 18, pp. 192-205, Mar-Apr 1994.
[25] J. G. Sled, A. P. Zijdenbos, and A. C. Evans, "A nonparametric method for automatic correction of intensity nonuniformity in MRI data," *IEEE Trans Med Imaging,* vol. 17, pp. 87-97, Feb 1998.
[26] A. P. Zijdenbos, A. C. Evans, F. Riahi, J. G. Sled, J. Chui, and V. Kollokian, "Automatic quantification of multiple sclerosis lesion volume using stereotaxic space " *Visualization in Biomedical Computing* vol. Volume 1131/1996, pp. 439-448, 1996.
[27] J. S. Kim, V. Singh, J. K. Lee, J. Lerch, Y. Ad-Dab'bagh, D. MacDonald, J. M. Lee, S. I. Kim, and A. C. Evans, "Automated 3-D extraction and evaluation of the inner and outer cortical surfaces using a Laplacian map and partial volume effect classification," *Neuroimage,* vol. 27, pp. 210-21, Aug 1 2005.
[28] J. Andrews and J. A. Sethian, "Fast marching methods for the continuous traveling salesman problem," *Proc Natl Acad Sci U S A,* vol. 104, pp. 1118-23, Jan 23 2007.
[29] M. E. Rettmann, X. Han, C. Xu, and J. L. Prince, "Automated sulcal segmentation using watersheds on the cortical surface," *Neuroimage,* vol. 15, pp. 329-44, Feb 2002.
[30] D. MacDonald, N. Kabani, D. Avis, and A. C. Evans, "Automated 3-D extraction of inner and outer surfaces of cerebral cortex from MRI," *Neuroimage,* vol. 12, pp. 340-56, Sep 2000.

ISBN: 978-988-19252-4-4
ISSN: 2078-0958 (Print); ISSN: 2078-0966 (Online)